Theor Chem Acc (2012) 131:1121
DOI 10.1007/s00214-012-1121-2

REGULAR ARTICLE

Theoretical studies of the effect of electron-withdrawing dicyanovinyl group on the electronic and charge-transport properties of fluorene-thiophene oligomers

Qing-Xiu Wu · Yun Geng · Yi Liao · Xiao-Dan Tang · Guo-Chun Yang · Zhong-Min Su

Received: 28 May 2011 / Accepted: 14 September 2011 / Published online: 25 February 2012

Abstract At the quantum-chemical level, we characterize some important parameters that control photoelectronic properties of three π-conjugated fluorene-thiophene oligomers namely, 2,7-di(2-thienyl)-9,9-dihexylfluorene, 2,5-Bis-(9H-fluorene-2-yl)-thieno[3,2-b]thiophene and 2,7-Bis [5-(1,1-dicyanovinyl)thiophene-2-yl]-9,9-di-n-hexylfluorene (**FTCN**). The geometric and electronic structures of these compounds in the ground and the lowest singlet excited states were studied using density function theory. By employing the incoherent transport model, the electron and hole mobilities were evaluated on a wide variety of nearest-neighbor charge transfer pathways. These results show that the chemical modifications by changing linkage mode or introducing the electron-withdrawing group could improve the charge transfer, especially for **FTCN**. Meanwhile, it is found that the packing effect weakens the emission intensity to some extent according to the simulations of photoluminescences of dimers.

Keywords Fluorene-thiophene oligomers · Optical property · Charge transport · DFT

1 Introduction

Fluorene-based conjugated oligomers have recently been investigated as preferred light-emitting materials over the corresponding polymers due to their well-defined structures, ease of purification, and absence of chain defects [1–9]. This fascinating family of conjugated materials could achieve full-color emission spanning almost the entire visible range by incorporating narrow gap comonomer, such as thiophene and its derivatives, into the large energy-gap oligofluorene backbone [10–13]. The advantage in combining both the thermal and chemical stability of oligofluorene with the adjustment of luminescence through facile chemical modification of thiophene fragment renders fluorene-thiophene oligomers promising active materials for a new generation of light-emitting diodes (LEDs). Unfortunately, shortcomings such as H-aggregation and/or excimer formation in the solid state will lead to unstable emission both in intensity and in color, and thereby limit their application [14, 15].

The usual strategy to control the aggregation of fluorene-thiophene oligomers is introduction of large steric hindrance substituents at C9-positon of the fluorene unit [15, 16]. In the past decade, 9,9-dialkyl substituted fluorene and fluorene-thiophene derivatives have been the subject of several studies [17–21]. Porzio and co-workers [22] have synthesized two fluorene-thiophene oligomers: linear alkyl chains linked to fluorene as a protecting group (**FT** [23], see Fig. 1) or a spiro-cyclopentane residue at the same positions. Both substituents allow the solubility and aggregation behavior of fluorene-thiophene oligomers to be

Electronic supplementary material The online version of this article (doi:10.1007/s00214-012-1121-2) contains supplementary material, which is available to authorized users.

Q.-X. Wu · Y. Geng · Y. Liao (✉) · X.-D. Tang · G.-C. Yang · Z.-M. Su (✉)
Faculty of Chemistry, Institute of Functional Material Chemistry, Northeast Normal University, Changchun 130024, China
e-mail: liaoy271@nenu.edu.cn

Z.-M. Su
e-mail: zmsu@nenu.edu.cn

Q.-X. Wu · Y. Liao
Department of Chemistry, Capital Normal University, Beijing 100048, China

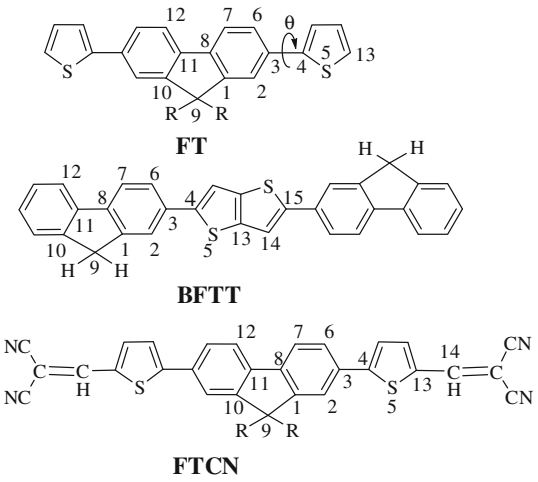

Fig. 1 Calculation models of **FT**, **BFTT**, and **FTCN**. Torsional angle was defined as: θ: C2–C3–C4–S5; R = C_6H_{13}

improved independently of their electronic properties. Meanwhile, the bulky substituents perpendicular to the molecular backbone also increase the intermolecular separation and thus suppress the charge mobility. A possible strategy to tune the charge-transport properties is to change the molecular packing into a π-stacking or herringbone motif, which will facilitate charge transfer through overlap of intermolecular orbitals [21, 24–27]. Kim [28] and coworkers reported a stable hole transporting material based on a structural combination of a fused bithiophene with fluorene (**BFTT**), which forms the well-known herringbone packing, and the charge mobility is increased to 0.01–0.02 $cm^2\ V^{-1}\ s^{-1}$ at room temperature. However, the well-known herringbone packing molecule of **BFTT** exhibits H-aggregation in addition to the keto-defect arising from oxidation at the C9 positions of fluorene fragment.

It seems difficult for luminescent materials to achieve a tradeoff between the good charge mobility and high quantum yield. Despite their high demand, there are relatively few reports on the oligofluorene–thiophenes that have good charge mobility while also maintaining high quantum yield. Recently, Liu et al. [23] synthesized a dicyanovinyl end-capped fluorene-thiophene co-oligomer **FTCN**. It is noticed that the charge-transport property could be improved by introduction of electron-withdrawing dicyanovinyl although large steric hindrance stemming from dialkyl side chain at C9 position of fluorene. The molecular packing structure resembles a honeycomb graphite, and the π-stacking of adjacent molecules is extended to form a highly fluorescent J-aggregates in the solid state. The dicyanovinyl group linked to thiophene is the only variation between **FT** and **FTCN** whose optoelectronic properties differ noticeably. It is, therefore, of great interest to answer the questions of how the electron-withdrawing substituents affect the charge mobilities and luminescent properties of oligofluorene–thiophenes and why **FTCN** without traditional cofacial or herringbone motif still exhibits high mobility.

To gain a better understanding of these issues, the reorganization energies and electronic couplings related to hole and electron transports as well as the luminescent properties of **FT**, **FTCN**, and **BFTT** are fully investigated by density function theory (DFT). As part of our ongoing efforts to establish the structure/optoelectronic property correlations [29–35], we address here the effect of chemical modification by changing linkage mode and introducing the electron-withdrawing unit on the transport and luminescence properties of oligofluorene–thiophenes. Theoretical analysis of the relationship between monomer structures and optoelectronic properties of materials can be expected to provide useful knowledge for the rational design and optimization of fluorene-based material that can enhance OLED performance.

2 Computational methods

All the quantum chemistry calculations were performed with the Gaussian 09 package [36]. To investigate the effect of different functionals on the molecular geometry, four density functionals including the B3LYP [20, 31, 37, 38], PBE1PBE (also called PBE0) [39–42], B3PW91 [43], and BP86 [44] methods were used with the 6-31G* basis set in the geometry optimization of the ground state (S_0) in case of **FT**. The selected bond lengths, bond angles, and corresponding experimental values are listed in Table S1, together with the sketch of relative errors of functional effects for bond lengths. There are little discrepancies among the bond lengths and bond angles for **FT** obtained from different functionals, and they are in good agreement with the experimental values except for the largest error of 4.5% for C–S bond evaluated from BP86. Considering the rationality of B3LYP functional reported in evaluation of geometric structures and spectra properties for oligofluorene-thiophene oligomers [19, 20, 45–49], B3LYP hybrid functional combined with the 6-31G* basis set was employed to optimize geometries for the other two molecules in this article (see Table S2). The basis set dependency of molecular geometry is described in supporting information (see Table S3).

There can be two different conformations of the **BFTT** with the *syn*- and *anti*-form (see Table S3). Preliminary calculations for the **BFTT** with B3LYP/6-31G* method give the two conformations very close in energies (ca. 0.06 kcal/mol), but the *syn*-structure is slightly more stable, so we choose it to perform further calculations.

The TD-DFT methodology [50, 51] is more reliable to optimize the lowest singlet excited state geometry (S_1)

[52–57] than the single-excitation configuration interaction (CIS) [58] method. Based on the S_0 state and S_1 equilibrium state structure, TD-B3LYP/6-31G* was employed to simulate the absorption and emission spectra of all compounds. The resulting transition energies are in excellent agreement with the corresponding experimental date.

Generally, the incoherent hopping model is employed to describe the charge-transport properties of organic materials. Each hopping step can be described as a self-exchange electron transfer from a charged (and relaxed) molecule to an adjacent neutral molecule. The rate of charge transfer is expressed by the semiclassical Marcus equation [59, 60]

$$k = \frac{V^2}{\hbar}\left(\frac{\pi}{\lambda k_B T}\right)^{\frac{1}{2}} \exp\left(-\frac{\lambda}{4k_B T}\right) \quad (1)$$

where $\hbar$, k_B, and T denote the Planck, Boltzmann constants and temperature, respectively. The intermolecular transfer integral (V) and the reorganization energy (λ) are two major parameters that determine the electron transfer rate. Here, λ reflects the geometric changes when going from the neutral to the charged state in the molecules. It can be regarded as a sum of two relaxation energy terms [61, 62]: $\lambda = \lambda_1 + \lambda_2$, as depicted in Fig. 2. However, theoretical calculations show that all these molecules exhibit inter-ring torsional angles in the gas phase, in contrast to the quasi-planar structures observed in the solid state. In order to be consistent with the crystal geometries, we constrain these molecules to planar geometries during the calculation process of the reorganization energies [63] using DFT method at the B3LYP/6-31G* level. At a fixed temperature (T), the drift mobility is expressed as the Einstein relation

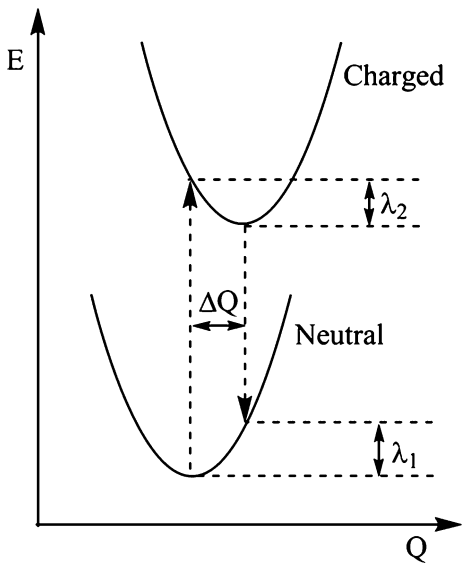

Fig. 2 Schematic description of the reorganization energy calculation

$$\mu = \frac{e}{k_B T} D \quad (2)$$

where e is the electronic charge, D is the diffusion coefficient, which is related to the charge-transfer rate k, and it can be approximately evaluated as [64–66]

$$D = \frac{1}{2d}\sum_i r_i^2 k_i P_i \quad (3)$$

$d = 3$ is the dimensionality. i represents a specific hopping pathway with r_i being the hopping centroid-to-centroid distance. Here, we assume that the charge hopping occurs only between nearest-neighbor molecules. P_i is the relative probability for charge carrier to a particular ith neighbor

$$P_i = k_i / \sum_i k_i \quad (4)$$

The intermolecular transfer integrals, characterizing the strength of electronic coupling between the two adjacent molecules, are obtained from the direct dimer Hamiltonian evaluation method [66–69] and can be written as

$$V = \left\langle \Phi^{0,\text{site1}}_{\text{LUMO/HOMO}} | F | \Phi^{0,\text{site2}}_{\text{LUMO/HOMO}} \right\rangle \quad (5)$$

where $\Phi^{0,\text{site1}}_{\text{LUMO/HOMO}}$ and $\Phi^{0,\text{site2}}_{\text{LUMO/HOMO}}$ represent the LUMOs/HOMOs of isolated molecules 1 and 2, respectively, and F is the Fock operator for the dimer with a density matrix from the noninteracting dimer of $F = SC\varepsilon C^{-1}$, where S is the intermolecular overlap matrix and C and ε are the molecular orbital coefficients and energies from one-step diagonalization without iteration. We employed the information of orbitals obtained using the B3LYP functional [70] in Gaussian 09 program to evaluate the values of transfer integrals for all hopping pathways by using our own developed program.

3 Results and discussion

3.1 Molecular geometries in ground- and excited-singlet state

The chemical structures of the oligofluorene-thiophene oligomers **FT**, **BFTT**, and **FTCN** are shown in Fig. 1. The selected optimized geometry parameters in their S_0 and S_1 states with B3LYP/6-31G* associated with experimental date are summarized in Table 1. For all molecules, the calculated bond lengths and bond angles are in good agreement with the X-ray measurement, and the deviations between computational and experimental results are within 0.08 Å and 0.8°, respectively. Differing from the quasi-planar structure observed in experimental measurements in the solid state, our theoretical calculations reveal that there exists a torsion angle of about 26° around the inter-ring C-C for all systems. For fluorene-thiophene oligomers

Table 1 Optimized geometries of S_0 and S_1 states for the three molecules as well as the corresponding experimental date

Parameters	**FT**			**BFTT**			**FTCN**		
	S_0	Exp.[22]	S_1	S_0	Exp.[28]	S_1	S_0	Exp.[23]	S_1
Bond distances (Å)									
C3–C4	1.467	1.469	1.433	1.465	1.464	1.423	1.462	1.457	1.436
C8–C11	1.464	1.464	1.422	1.467	1.468	1.452	1.460	1.438	1.430
C4–S5	1.756	1.689	1.776	1.774	1.721	1.866	1.746	1.724	1.763
S5–C13	1.734	1.693	1.735	1.744	1.668	1.815	1.757	1.727	1.760
Dihedral angles (°)									
C2–C3–C4–S5	27.3	4.9	0.0	26.5	0.6	0.0	25.2	1.0	0.5

TFT, a slightly larger torsion angle between thiophene and fluorene (ca. 39°) in fluorene-thiophene oligomer has been reported based on HF/6-31G* method [71]. More recently, Hannongbua and Nakatsuji [45] revealed from their B3LYP/6-31G* calculations that the torsion angel between fluorene and thiophene in **FT** is about 27°, just as our results predicted. Such a discrepancy in the torsion angle between gas-phase calculations and condensed-phase measurements is normally ascribed to the intermolecular packing in the solid state [72]. In order to assess the stacking effect on the molecular structure, a packing model of **BFTT** is selected from X-ray structure in such a way that the nearest four neighboring molecules are retained surrounding the center molecule. The corresponding inter-ring dihedral angle of **BFTT** decreases from 26° to 15° (see Table S2). If increasing the numbers of the stacking molecule surrounding the center molecule, we predict that the dihedral angle may reduce much better. Therefore, intermolecular packing can primarily account for the discrepancy. Another intriguing possibility is that planar geometry may represent the rotationally averaged position between the fluorene and thiophene ring [73].

For the ground state, our calculations reveal that the introduction of the fused bithiophene and electron-withdrawing dicyanovinyl group has little effect on the bond lengths of the fluorenyl fragment, but shorten the interring bond C3–C4 in the progressive sequence of **FT** (1.467 Å) > **BFTT** (1.465 Å) > **FTCN** (1.462 Å). Comparing the geometrical structures in the lowest singlet state with those in ground state, there are significant variations in the bond lengths (see Table S2) and interring torsion angels θ for all compounds (Table 1). The geometry structures have a strong coplanar tendency in S_1 states with the torsional angle close to 0°. In addition, the inter-ring bond distance (C3–C4) is shorter in the S_1 state than in the S_0 state for each molecule. This evident geometry twist between S_0 and S_1 states will bring the large relaxation energy, especially for **BFTT**.

3.2 Frontier molecular orbitals and electronic spectra

For describing the optical and electronic characteristics, it is helpful to investigate the highest occupied molecular orbital (HOMO), the lowest unoccupied molecular orbital (LUMO), and the energy gap defined as energy difference between the HOMO and LUMO levels (shown in Fig. 3). As can be seen from Fig. 3, both the HOMOs and LUMOs in all systems hold π orbital features and are delocalized over the whole aromatic backbone. Compared with **FT**, the elongation of π-conjugation of **BFTT** slightly increases the HOMO level and decreases the LUMO level, thus leading to a moderate contraction of the HOMO-LUMO gap by 0.34 eV. While the electron-withdrawing substitution linked to thiophene moieties significantly lowers the LUMO energy more than the HOMO level. This results in a HOMO-LUMO gap for **FTCN** of roughly 2.78 eV, almost one electronvolt smaller than that of **FT**. The reduction in the energy gap observed when going from **FT** to **BFTT** and to **FTCN** will impact their optical properties.

The relevant parameters such as transition energies and oscillator strengths for each compound are listed in

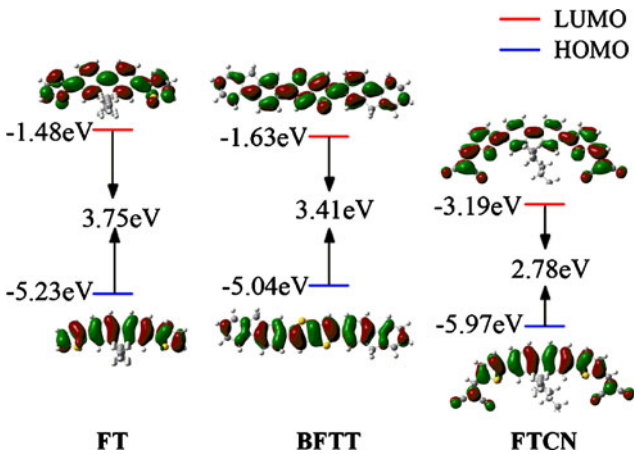

Fig. 3 The frontier molecular orbitals of **FT**, **BFTT**, and **FTCN** according to DFT calculations at the B3LYP/6-31G* level

Table 2 The maximal absorption (λ_{max}, $S_0 \rightarrow S_1$) and emission ($S_1 \rightarrow S_0$) by TD-DFT for FT, BFTT, and FTCN at the S_0 state (B3LYP/6-31G*) and S_1 state (TD-B3LYP/6-31G*) geometries, respectively, together with the corresponding experimental date

Molecule	Absorption				Stokes shift (nm)	Emission			
	$\lambda_{max,\ abs}$(nm)	E(eV)	f	Exp.		λ_{emi}(nm)	E(eV)	f	Exp.
FT	360	3.44	1.18	357[a]	63	423 (457)	2.93 (2.71)	1.35 (0.15 × 10^{-1})	442[a]
BFTT	401	3.09	1.98	430[b]	100	501 (559)	2.47 (2.22)	2.19 (0.00)	500[b]
FTCN	492	2.52	1.39	483[c]	63	555 (616)	2.23 (2.01)	1.66 (0.86 × 10^{-2})	571[c]

E and f represent vertical excited energy and oscillator strength, respectively

[a] Measured in film (Ref. [23])

[b] Measured in about 50-nm-thick film for absorption and about 300-nm-thick for emission (Ref. [28]). The data shown in parenthesis represent the maximal emission of the dimers of these corresponding compounds

[c] Measured in film (Ref. [23])

Table 2. It can be seen that the calculated data for maximum absorptions and emissions are compatible with their experimental counterparts. The lowest-energy excitations evaluated for all systems are mainly associated with transitions from corresponding HOMOs to the LUMOs, as the coefficients in the configuration interaction wave functions are up to 0.70. The absorption maximum follows the order **FT** (360 nm) < **BFTT** (401 nm) < **FTCN** (492 nm), well consistent with the changing trend of energy gap.

Similarly, the bathochromic shift passing from **FT** to **BFTT** and to **FTCN** is reproduced in the $\pi \rightarrow \pi^*$ emission peak related to the $S_1 \rightarrow S_0$ transitions. The emission maximum of each single compound is predicted to be more intense compared with that of absorption, with the Stokes shifts of 63, 100, 63 nm for **FT**, **BFTT,** and **FTCN**, respectively. Figure 4 shows the vertical excitation and relaxation energies (eV) for **BFTT** and **FTCN**. The large Stokes shift for **BFTT** could be attributed to the big relaxation energies of 0.61 eV.

Compared to **FT**, enhancements in the oscillator strengths of substituted **BFTT** and **FTCN**, especially for the **BFTT**, are detected both in $S_0 \rightarrow S_1$ and $S_1 \rightarrow S_0$ transition. The increased intensity in emission, desirable for improvement of quantum efficiency, can be ascribed to the elongation of the π-delocalization along the molecular long axis. The situation is exactly reverse when the packing effect is taken into account (see Fig. 2), which obviously weakens the emission intensity, especially for the **BFTT** that the packing effect leads to quenching of luminescence.

3.3 Ionization potential, electron affinity, and reorganization energy

The performance of OLED also depends on the balanced injection and transport of holes and electrons into the emitter layer. In general, conjugated molecule having a low ionization potential (IP) (or high electron affinity EA) will facilitate the injection of holes (electrons) into the devices with a low initial driving voltage. The calculated vertical and adiabatic IPs and EAs for all molecules studied in this paper are listed in Table 3. Upon going from **FT** to **BFTT**, the IPs decrease by about 0.3 eV, and the EAs increase by 0.3 eV; the respective changes suggest that the extension of conjugated length will simultaneously enhance the injection of positive and negative charges. However, the introduction of electron-withdrawing dicyanovinyl unit into **FT** contributes to moderately elevating the IPs by 0.6 eV and markedly increasing the EAs by about 2.0 eV, which means that the electron-pull effect greatly improves the injection ability of electrons.

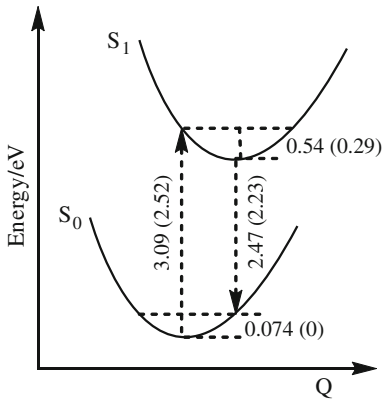

Fig. 4 The transition and relaxation energies (eV) calculated with TD-B3LYP/6-31G* for **BFTT** and **FTCN** (in *parenthesis*)

Table 3 Ionization potentials, electronic affinities, and reorganization energies (eV) for **FT**, **BFTT**, and **FTCN** calculated by DFT//B3LYP/6-31G*

Molecule	IP(v)	IP(a)	EA(v)	EA(a)	λ_{hole}	$\lambda_{electron}$
FT	6.35	6.24	0.38	0.49	0.23	0.22
BFTT	6.06	5.96	0.67	0.79	0.22	0.24
FTCN	6.91	6.84	2.25	2.34	0.14	0.19

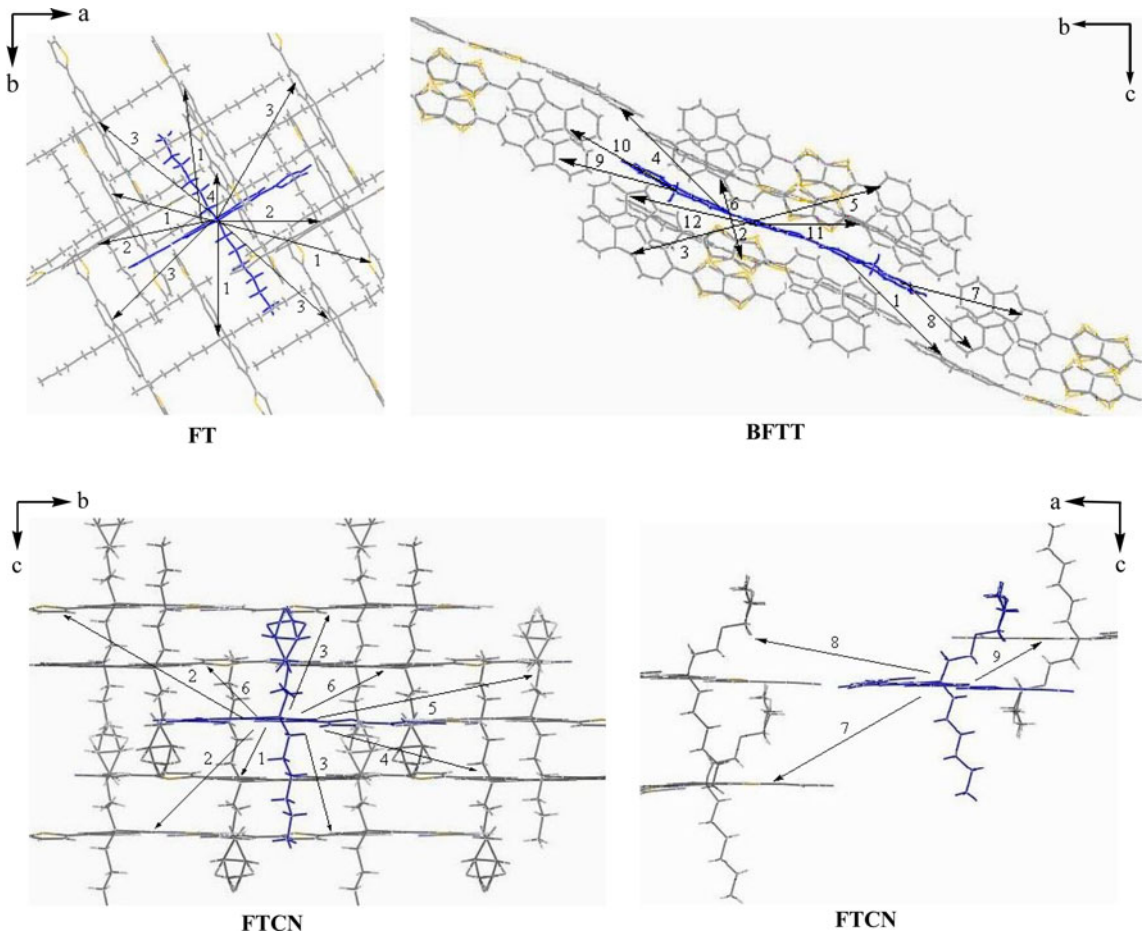

Fig. 5 Carrier transport pathways of **FT**, **BFTT**, and **FTCN**

One important parameter that determines the charge mobility is the reorganization energy, which comes from geometry relaxations as the electron or hole transfers from one molecule to the neighboring one. Our calculation results indicate that both the hole reorganization energy λ_{hole} (0.23 eV) and the electron reorganization energy $\lambda_{electron}$ (0.22 eV, see Table 3) of **FT** are very close to those of **BFTT** (0.22 eV for the λ_{hole} and 0.24 eV for the $\lambda_{electron}$), which can be ascribed to the similar molecular distortions of both compounds from neutral- to charged state (shown in Figure S1). The λ_{hole} (0.14 eV) and $\lambda_{electron}$ (0.19 eV) of **FTCN** are much smaller than those of the others mainly because of the weaker geometry relaxation. Generally, small reorganization energy is in favor of speeding up to the charge-transport process according to the (Eq. 1).

3.4 Charge transport

Besides λ, another factor that plays an important role in determining the charge carrier mobility is the transfer integral V. For **FT**, **BFTT**, and **FTCN**, all carrier hopping pathways obtained directly from their X-ray data are displayed in Fig. 5, and the corresponding transfer integrals of all systems calculated by the direct coupling method (Eq. 5) through these pathways are shown in Table 4. The maximum transfer integrals V_{max} of hole and electron for each compound are emphasized with bold font. It is generally accepted that the transfer integral between two molecules correlates to some extent to the intermolecular interaction. Therefore, the intermolecular interactions of main hopping pathways for all compounds were evaluated by natural bond orbital (NBO) analysis [29] and listed in Table 5.

For **FT**, the largest transfer integrals of the hole and electron are in the pathway 3 with the value of 6.79 and 4.41 meV, respectively, which are almost one order of magnitude smaller than those of **BFTT** (18.8 meV for V_{hole} in pathway 3 and 36.7 meV for $V_{electron}$ in pathway 11). Since the V_{max} makes the major contribution to the carrier transfer, detailed comparison of the intermolecular interactions in the maximum transporting pathway between **FT**

Table 4 The maximal transfer integral values V (eV) of hole and electron for **FT**, **BFTT**, and **FTCN** compounds

Molecular	Pathway	Dimer CM distance (Å)	V_{hole}	$V_{electron}$
FT	1	9.76	4.75×10^{-3}	9.31×10^{-4}
	2	9.80	3.60×10^{-4}	9.71×10^{-4}
	3	11.71	$\mathbf{6.79 \times 10^{-3}}$	$\mathbf{4.41 \times 10^{-3}}$
	4	10.25	3.41×10^{-4}	7.6×10^{-10}
BFTT	1	23.01	2.59×10^{-4}	4.67×10^{-4}
	2	5.06	4.14×10^{-3}	2.12×10^{-3}
	3	5.24	$\mathbf{1.88 \times 10^{-2}}$	3.04×10^{-2}
	5	5.24	1.52×10^{-2}	2.99×10^{-2}
	6	5.06	9.92×10^{-5}	1.54×10^{-2}
	7	24.66	8.16×10^{-4}	7.96×10^{-5}
	8	24.09	2.03×10^{-3}	2.11×10^{-3}
	11	5.77	2.50×10^{-3}	$\mathbf{3.67 \times 10^{-2}}$
	12	5.77	1.79×10^{-3}	3.31×10^{-2}
FTCN	1	9.58	$\mathbf{6.29 \times 10^{-2}}$	9.68×10^{-3}
	4	16.05	2.70×10^{-2}	$\mathbf{3.39 \times 10^{-2}}$
	5	15.36	6.96×10^{-4}	9.40×10^{-4}
	6	12.39	2.03×10^{-2}	2.90×10^{-2}
	7	17.29	4.70×10^{-4}	7.22×10^{-4}
	8	18.45	5.97×10^{-4}	8.20×10^{-4}
	9	7.93	2.88×10^{-2}	2.43×10^{-2}
	10	13.74	3.39×10^{-2}	1.57×10^{-2}

and **BFTT** would be helpful for understanding the relationship between chemical modification and the transport property of this series of materials. As can be seen from Table 5, the **FT** dimer in the pathway 3 adopts an edge-to-face configuration, and the primary intermolecular interaction is originated from the CH···S contact between lone pair (LP) of sulfur in the thiophene ring and the adjacent pendant alkyl. When the large side chain at C9 position is replaced by H atom, planar **BFTT** can achieve close packing in a herringbone arrangement, which consists of face-to-face stacking besides edge-to-face packing. For **BFTT**, the representative CH···π and additional CH···S interactions are found between adjacent edge-to-face stacked molecules, companying with the S···π [74] and CH···π/S interactions existing between neighboring face-to-face molecules. We may infer that removal of large steric hindrance of dialkyl substituents in **BFTT** could effectively strengthen the intermolecular interactions, and then enhance its transfer integrals. The drift mobilities (μ) calculated from Einstein-Smoluchowski relation are listed in Table 6. The hole mobility of **BFTT** (0.022 $cm^2\ V^{-1}\ s^{-1}$) is reasonably close to the experimental datum [28]. For **BFTT**, the μ_{hole} and $\mu_{electron}$ (0.071 $cm^2\ V^{-1}\ s^{-1}$) are about two times larger than those of **FT**. Considering their similar reorganization energies stated above, the higher

Table 6 The calculated carrier mobilities ($cm^2\ V^{-1}\ s^{-1}$) for both hole (μ_h) and electron (μ_e) of **FT**, **FTCN**, and **BFTT**

Compound	μ_{hole}	$\mu_{electron}$	Exp. (μ_{hole})
FT	1.2×10^{-2}	6.7×10^{-3}	–
BFTT	2.2×10^{-2}	7.1×10^{-2}	0.01–0.02 (0.009–0.01)[28]
FTCN	19.1×10^{-1}	6.2×10^{-1}	–

Table 5 Natural bond orbital (NBO) analysis of intermolecular interactions in these molecules

CH…π

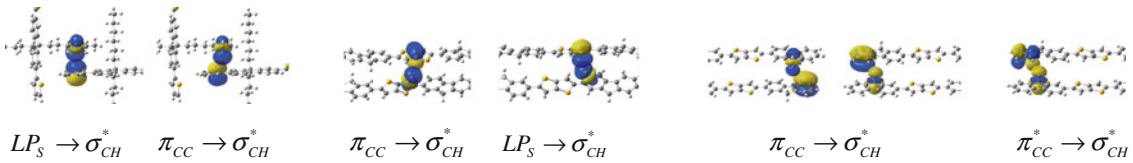

FT-path3 **BFTT**- edge-to-face **BFTT**- face-to-face

S…π π…π Hydrogen Bond

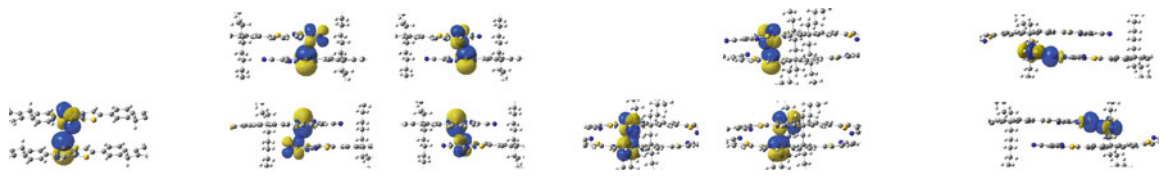

BFTT- face-to-face **FTCN**- cross-like packing **FTCN**- face-to-face **FTCN**- cross-like packing

mobilities of **BFTT** are ascribed to its larger transfer integrals.

When electron-withdrawing dicyanovinyl groups are connected to thiophene moieties in **FT**, excessive intermolecular interactions are introduced among neighboring molecules in **FTCN**. In addition to π-π interactions within the quasi-parallel molecules, the intermolecular interactions in **FTCN** are highly strengthened by CH···N hydrogen bonds and π-type (S···CN/CC) contacts along horizontal and vertical directions, respectively, in the cross-like packing motif. The predicted V_{max} for electron (33.9 meV) and hole (62.9 meV) of **FTCN** with large side chain are comparable to or even slightly larger than those of **BFTT** and one order of magnitude higher than corresponding values of **FT**. Comparing with the other two compounds, the large transfer integrals and small reorganization energies of **FTCN** greatly enhance the charge transfer according to the Marcus rate formula. Thus, both hole (1.91 $cm^2\ V^{-1}\ s^{-1}$) and electron (0.62 $cm^2\ V^{-1}\ s^{-1}$) drift mobilities (see Table 6) of **FTCN** are the largest one among the three molecules investigated. As mentioned above, the transfer integrals of **BFTT** and **FTCN** are relatively close, but the calculated mobilites differ by one order of magnitude. It is the reorganization energy that really makes the difference.

4 Conclusions

According to the quantum-chemical results, it was found that the chemical modifications by changing linkage mode or introducing the electron-pulling group could improve the charge transfer to some extent. However, the packing effect weakens the emission intensity, especially for the **BFTT**. Although the packing style of **FTCN** also decrease the oscillator strength of emission, the present of electron-withdrawing unit obviously increases the transfer integral, decreases the reorganization energy, and consequently enhances the charge transport.

Acknowledgments The authors gratefully acknowledge financial support from NCET 11224010026, NSFC 20903020, 973 Program (2009CB623605), and Scientific Research Common Program of Beijing Municipal Education Commission (No. KM201110028007).

References

1. Culligan SW, Geng Y, Chen SH, Klubek K, Vaeth KM, Tang CW (2003) Adv Mater 15:1176. doi:10.1002/adma.200304972
2. Wu CC, Lin YT, Wong KT, Chen RT, Chien YY (2004) Adv Mater 16:61. doi:10.1002/adma.200305619
3. Lu HH, Liu CY, Chang CH, Chen SA (2007) Adv Mater 19:2574. doi:10.1002/adma.200602632
4. Aharon E, Albo A, Kalina M, Frey GL (2006) Adv Fucnt Mater 16:980. doi:10.1002/adfm.200500458
5. van Woudenbergh T, Wildeman J, Blom PWM, Bastiaansen JJAM, Langeveld-Vos BMW (2004) Adv Fucnt Mater 14:677. doi:10.1002/adfm.200305178
6. Cocherel N, Poriel C, Rault-Berthelot J, Barrière F, Audebrand N, Slawin Alexandra MZ, Vignau L (2008) Chem Eur J 14:11328. doi:10.1002/chem.200801428
7. Liu J, Zou J, Yang W, Wu H, Li C, Zhang B, Peng J, Cao Y (2008) Chem Mater 20:4499. doi:10.1021/cm800129h
8. Jacob J, Sax S, Piok T, List EJW, Grimsdale AC, Müllen K (2004) J Am Chem Soc 126:6987. doi:10.1021/ja0398823
9. Wu PL, Feng XJ, Tam HL, Wong MS, Cheah KW (2008) J Am Chem Soc 131:886. doi:10.1021/ja806703v
10. Ranger M, Rondeau D, Leclerc M (1997) Macromolecules 30:7686. doi:10.1021/ma970920a
11. Donat-Bouillud A, Levesque I, Tao Y, D'Iorio M, Beaupre S, Blondin P, Ranger M, Bouchard J, Leclerc M (2000) Chem Mater 12:1931. doi:10.1021/cm0001298
12. Liu B, Yu WL, Lai YH, Huang W (2001) Chem Mater 13:1984. doi:10.1021/cm0007048
13. Li ZH, Wong MS, Fukutani H, Tao Y (2005) Chem Mater 17:5032. doi:10.1021/cm051163v
14. Grell M, Bradley DDC, Ungar G, Hill J, Whitehead KS (1999) Macromolecules 32:5810. doi:10.1021/ma990741o
15. Setayesh S, Grimsdale AC, Weil T, Enkelmann V, Müllen K, Meghdadi F, List EJW, Leising G (2001) J Am Chem Soc 123:946. doi:10.1021/ja0031220
16. Wong KT, Chien YY, Chen RT, Wang CF, Lin YT, Chiang HH, Hsieh PY, Wu CC, Chou CH, Su YO, Lee GH, Peng SM (2002) J Am Chem Soc 124:11576. doi:10.1021/ja0269587
17. Tang W, Ke L, Tan L, Lin T, Kietzke T, Chen ZK (2007) Macromolecules 40:6164. doi:10.1021/ma070575h
18. Pal B, Yen WC, Yang JS, Su WF (2007) Macromolecules 40:8189. doi:10.1021/ma071126k
19. Du C, Ye S, Chen J, Guo Y, Liu Y, Lu K, Liu Y, Qi T, Gao X, Shuai Z, Yu G (2009) Chem Eur J 15:8275. doi:10.1002/chem.200900860
20. Chen C-H, Hsu Y-C, Chou H-H, Thomas KRJ, Lin Jiann T, Hsu C-P (2010) Chem Eur J 16:3184. doi:10.1002/chem.200903151
21. Zeng L, Yan F, Wei SKH, Culligan SW, Chen SH (2009) Adv Fucnt Mater 19:1978. doi:10.1002/adfm.200900101
22. Destri S, Pasini M, Botta C, Porzio W, Bertini F, Marchio L (2002) J Mater Chem 12:924. doi:10.1039/b109089p
23. Qi T, Liu Y, Qiu W, Zhang H, Gao X, Liu Y, Lu K, Du C, Yu G, Zhu D (2008) J Mater Chem 18:1131. doi:10.1039/b715920j
24. Tang ML, Roberts ME, Locklin JJ, Ling MM, Meng H, Bao Z (2006) Chem Mater 18:6250. doi:10.1021/cm0623514
25. Meng H, Bao Z, Lovinger AJ, Wang BC, Mujsce AM (2001) J Am Chem Soc 123:9214. doi:10.1021/ja016525o
26. Meng H, Zheng J, Lovinger AJ, Wang BC, Van Patten PG, Bao Z (2003) Chem Mater 15:1778. doi:10.1021/cm020866z
27. Surin M, Sonar P, Grimsdale AC, Mullen K, Feyter SD, Habuchi S, Sarzi S, Braeken E, Heyen AV, Auweraer MVd, Schryver FCD, Cavallini M, Moulin J-F, Biscarini F, Femoni C, Lazzaroni R, Leclere P (2007) J Mater Chem 17:728. doi:10.1039/b610132a
28. Noh YY, Azumi R, Goto M, Jung BJ, Lim E, Shim HK, Yoshida Y, Yase K, Kim DY (2005) Chem Mater 17:3861. doi:10.1021/cm0504889
29. Liao Y, Ma J (2008) Organometallics 27:4636. doi:10.1021/om8001697
30. Yang G, Liao Y, Su Z, Zhang H, Wang Y (2006) J Phys Chem A 110:8758. doi:10.1021/jp061286i
31. Gao HZ, Qin CS, Zhang HY, Wu SX, Su ZM, Wang Y (2008) J Phys Chem A 112:9097. doi:10.1021/jp804308e

32. Geng Y, Wang JP, Wu SX, Li HB, Yu F, Yang GC, Gao HZ, Su ZM (2011) J Mater Chem 21:134. doi:10.1039/c0jm02119a
33. Geng Y, Li H, Wu S, Duan Y, Su Z, Liao Y (2011) Theo Chem Acc 129:247. doi:10.1007/s00214-011-0928-6
34. Tang X, Gao H, Geng Y, Liao Y, Su Z (2010) Chem J Chin Univ 31:766
35. Yang G, Si Y, Geng Y, Yu F, Wu Q, Su Z (2011) Theo Chem Acc 128:257. doi:10.1007/s00214-010-0841-4
36. Frisch MJ, Trucks GW, Schlegel HB, Scuseria GE, Robb MA, Cheeseman JR, Scalmani G, Barone V, Mennucci B, Petersson GA, Nakatsuji H, Caricato M, Li X, Hratchian HP, Izmaylov AF, Bloino J, Zheng G, Sonnenberg JL, Hada M, Ehara M, Toyota K, Fukuda R, Hasegawa J, Ishida M, Nakajima T, Honda Y, Kitao O, Nakai H, Vreven T, Montgomery JA Jr, Peralta JE, Ogliaro F, Bearpark M, Heyd JJ, Brothers E, Kudin KN, Staroverov VN, Kobayashi R, Normand J, Raghavachari K, Rendell A, Burant JC, Iyengar SS, Tomasi J, Cossi M, Rega N, Millam JM, Klene M, Knox JE, Cross JB, Bakken V, Adamo C, Jaramillo J, Gomperts R, Stratmann RE, Yazyev O, Austin AJ, Cammi R, Pomelli C, Ochterski JW, Martin RL, Morokuma K, Zakrzewski VG, Voth GA, Salvador P, Dannenberg JJ, Dapprich S, Daniels AD, Farkas O, Foresman JB, Ortiz JV, Cioslowski J, Fox DJ (2009) Gaussian 09, Revision A.02. Gaussian, Inc., Wallingford
37. Becke AD (1993) J Chem Phys 98:5648. doi:10.1063/1.464913
38. Fortrie R, Chermette H (2007) J Chem Theory Comput 3:852. doi:10.1021/ct600369b
39. Adamo C, Barone V (1999) J Chem Phys 110:6158
40. Muhammad S, Janjua MRSA, Su Z (2009) J Phys Chem C 113:12551. doi:10.1021/jp903075s
41. Muhammad S, Xu H, Liao Y, Kan Y, Su Z (2009) J Am Chem Soc 131:11833. doi:10.1021/ja9032023
42. Jacquemin D, Preat J, Wathelet V, Fontaine M, Perpète EA (2006) J Am Chem Soc 128:2072. doi:10.1021/ja056676h
43. McClure SA, Buriak JM, DiLabio GA (2010) J Phys Chem C 114:10952. doi:10.1021/jp912122q
44. Gahungu G, Zhang B, Zhang J (2007) J Phys Chem C 111:4838. doi:10.1021/jp067067e
45. Poolmee P, Ehara M, Hannongbua S, Nakatsuji H (2005) Polymer 46:6474. doi:10.1016/j.polymer.2005.03.120
46. Gong Z, Lagowski JB (2007) Int J Quantum Chem 107:159. doi:10.1002/qua.21030
47. Liu YL, Feng JK, Ren AM (2008) J Phys Chem A 112:3157. doi:10.1021/jp7104067
48. Ran XQ, Feng JK, Liu YL, Ren AM, Zou LY, Sun CC (2008) J Phys Chem A 112:10904. doi:10.1021/jp805553e
49. Poolmee P, Hannongbua S (2010) J Comput Chem 31:1945. doi:10.1002/jcc.21490
50. Runge E, Gross EKU (1984) Phys Rev Lett 52:997. doi:10.1103/PhysRevLett.52.997
51. Bauernschmitt R, Ahlrichs R (1996) Chem Phys Lett 256:454
52. Dierksen M, Grimme S (2004) J Chem Phys 120:3544
53. Furche F, Ahlrichs R (2002) J Chem Phys 117:7433
54. Burcl R, Amos RD, Handy NC (2002) Chem Phys Lett 355:8
55. Teng YL, Kan YH, Su ZM, Liao Y, Yan LK, Yang YJ, Wang RS (2005) Int J Quantum Chem 103:775. doi:10.1002/qua.20491
56. Liao Y, Feng JK, Yang L, Ren AM, Zhang HX (2004) Organometallics 24:385. doi:10.1021/om0494317
57. Yang GC, Su T, Shi SQ, Su ZM, Zhang HY, Wang Y (2007) J Phys Chem A 111:2739. doi:10.1021/jp067685v
58. Foresman JB, Head-Gordon M, Pople JA, Frisch MJ (1992) J Phys Chem 96:135. doi:10.1021/j100180a030
59. Marcus RA (1993) Rev Mod Phys 65:599. doi:10.1103/RevModPhys.65.599
60. Balzani V, Juris A, Venturi M, Campagna S, Serroni S (1996) Chem Soc Rev 96:759. doi:10.1021/cr941154y
61. Coropceanu V, Malagoli M, da Silva Filho DA, Gruhn NE, Bill TG, Brédas JL (2002) Phys Rev Lett 89:275503. doi:10.1103/PhysRevLett.89.275503
62. Berlin YA, Hutchison GR, Rempala P, Ratner MA, Michl J (2003) J Phys Chem A 107:3970. doi:10.1021/jp034225i
63. Kjelstrup-Hansen J, Norton JE, da Silva Filho DA, Brédas JL, Rubahn HG (2009) Org Electron 10:1228. doi:10.1016/j.orgel.2009.06.015
64. Kuo MY, Chen HY, Chao I (2007) Chem Eur J 13:4750. doi:10.1002/chem.200601803
65. Wang Lj, Nan Gj, Yang Xd, Peng Q, Li Qk, Shuai Zg (2010) Chem Soc Rev 39:423. doi:10.1039/b816406c
66. Yang XD, Li QK, Shuai ZG (2007) Nanotechnology 18:424029. doi:10.1088/0957-4484/18/42/424029
67. Troisi A, Orlandi G (2001) Chem Phys Lett 344:509. doi:10.1016/S0009-2614(01)00792-8
68. Yang X, Wang L, Wang C, Long W, Shuai Z (2008) Chem Mater 20:3205. doi:10.1021/cm8002172
69. Yin S, Yi Y, Li Q, Yu G, Liu Y, Shuai Z (2006) J Phys Chem A 110:7138. doi:10.1021/jp057291o
70. Valeev EF, Coropceanu V, da Silva Filho DA, Salman S, Brédas J-L (2006) J Am Chem Soc 128:9882. doi:10.1021/ja061827h
71. Belletête M, Morin J-F, Beaupré S, Ranger M, Leclerc M, Durocher G (2001) Macromolecules 34:2288. doi:10.1021/ma001042a
72. Martínez F, Neculqueo G, Vásquez SO, Letelier R, Garland MT, Ibañez A, Bernède JC (2010) J Mol Struct 973:56. doi:10.1016/j.molstruc.2010.03.022
73. Perez-Jimenez AJ, Sancho-Garcia JC, Perez-Jorda JM (2005) J Chem Phys 123:134309. doi:10.1063/1.2043107
74. Yan S, Lee SJ, Kang S, Choi K-H, Rhee SK, Lee JY (2007) Bull Korean Chem Soc 28:959